

000 001 002 003 004 005 DUAL PRIVACY PROTECTION IN DECENTRALIZED 006 LEARNING 007 008 009

010 **Anonymous authors**
011 Paper under double-blind review
012
013
014
015
016
017
018
019
020
021
022
023
024
025
026
027
028
029

030 ABSTRACT 031

032 In decentralized learning systems, significant effort has been devoted to protecting
033 the privacy of each agent’s local data or gradients. However, the shared model pa-
034 rameters themselves can also reveal sensitive information about the targets, which
035 the network is estimating. **While differential privacy-based decentralized learning**
036 **can protect network estimates, using excessively large privacy noise variance will**
037 **significantly reduce the accuracy of network estimates.** To this end, we propose a
038 dual-protection framework for decentralized learning. Within this framework, we
039 develop two privacy-preserving algorithms, named DSG-RMS and EDSG-RMS.
040 Different from existing differential privacy distributed learning methods, the de-
041 signed algorithms simultaneously obscure the network’s estimated values and lo-
042 cal gradients, by adding a protective perturbation vector at each update and by
043 using random matrix-step-sizes. Then, we establish convergence guarantees for
044 both algorithms under convex objectives. In particular, our error bound and pri-
045 vacy analysis highlight how the variance of the random matrix-step-sizes affects
046 both algorithmic performance and the privacy of local gradients. **Despite using**
047 **large-variance random step-sizes for stronger gradient privacy, the network’s esti-**
048 **mation accuracy in our algorithms can still be improved by choosing a sufficiently**
049 **small algorithmic parameter γ .** Finally, we validate the practical effectiveness
050 of the proposed algorithms through extensive experiments across diverse applica-
051 tions, including distributed filtering, distributed learning, and target localization.
052
053

1 INTRODUCTION

034 In decentralized learning, a key task is estimating global parameters from local data across dis-
035 tributed agents, as in cooperative spectrum sensing, multi-target localization, and bio-inspired sys-
036 tems Sayed (2022). Agents collaborate via incremental, consensus, or diffusion strategies, exchang-
037 ing intermediate results or gradients. Such exchanges, however, can compromise privacy, since
038 gradients may reveal sensitive local training data Shokri & Shmatikov (2015); Ma et al. (2023).

039 To address privacy concerns in decentralized learning, various protective mechanisms have been
040 developed. Cryptographic approaches—such as secret sharing Li et al. (2019a), secure multi-party
041 computation Mohassel & Zhang (2017), and homomorphic encryption Lu & Zhu (2018); Ruan et al.
042 (2019); Fu et al. (2024)—offer strong privacy guarantees, **but incur substantial computational and**
043 **communication overhead.** System decomposition methods enhance privacy by constructing virtual
044 agent and restructuring local objective; **however, they introduce additional computational complex-**
045 **ity Zhang et al. (2018).** Differential privacy (DP) provides a lightweight alternative by injecting zero-
046 mean noise into shared quantities He et al. (2018); Wei et al. (2020); Hu et al. (2024). It has been
047 successfully integrated into ADMM-based distributed algorithms and gradient tracking frameworks
048 across both directed and undirected network topologies Zhang & Zhu (2016); Huang et al. (2024);
049 Zhu et al. (2018); Lü et al. (2020). Another class of noise-based methods applies multiplicative noise
050 to modify local measurements, as seen in Harrane et al. (2016); however, its effectiveness relies on
051 the restrictive assumption that local optima coincide with the global solution, and it significantly
052 increases communication overhead. The fundamental challenge of DP-based decentralized learning
053 algorithms lies in the inherent trade-off between privacy and network accuracy: stronger privacy
054 requires more noise, which in turn degrades the quality of network estimated parameters. Recent
055 work has sought to improve this trade-off through techniques such as variance-decaying noise, zero-
056 sum noise, and graph-homomorphic noise, while achieving (ϵ, δ) -differential privacy Ding et al.

(2021); Rizk et al. (2023). However, in distributed consensus learning settings, it faces a critical phenomenon: As the iteration proceeds, the transmitted signals become nearly identical—for example, in decentralized stochastic gradient algorithm. When the added noise has a small variance—but sufficient to preserve gradient—an adversary may still recover the mean value of transmitted data by applying statistical operations such as sliding-window averaging. This privacy risk is particularly acute in wireless sensor localization networks, where the shared data typically contains sensitive location information Piperigkos et al. (2021); Shi et al. (2022).

In this paper, we focus on the privacy risks related to the exposure of network estimated values and local gradients/data during information exchange. To address these concerns, we introduce a novel dual-protection privacy-enhancing framework that integrates two key components: a non-zero protection vector and a random matrix-step-sizes (RMS) mechanism. By embedding this framework into the decentralized stochastic gradient (DSG) algorithm and exact diffusion variant (EDSG), we develop two advanced privacy-preserving methods: DSG-RMS and EDSG-RMS. Then, we conduct a comprehensive convergence analysis of the proposed algorithms under convex objective functions. The theoretical results demonstrate that both DSG-RMS and EDSG-RMS achieve convergence to a neighborhood of the optimal solution. Furthermore, we examine the effect of random matrix-step-sizes and protection vectors on algorithmic performance. Notably, **increasing the variance of the random step-sizes enhances gradient privacy but simultaneously amplifies sensitivity to data heterogeneity, resulting in looser error bounds and degraded network estimation accuracy**. Our main contributions are summarized as follows:

- We propose two novel algorithms for decentralized learning: DSG-RMS and EDSG-RMS. The EDSG-RMS variant is particularly well-suited for settings with heterogeneous data across devices.
- We provide rigorous convergence analyses for both algorithms under convex and strongly convex objective functions. This analysis reveals how specific parameter choices influence the overall network performance. **Even when a large variance in the random matrix-step-sizes is used to ensure strong privacy of the gradient, the proposed algorithms can improve the network’s estimation accuracy by reducing the parameter γ .**
- We conduct comprehensive experiments, and the results confirm the effectiveness of our methods. We further evaluate their ability to preserve privacy, showing that both network estimates and individual data remain well protected.

2 RELATED WORKS

As discussed earlier, the PD offers a way to protect shared gradient information by adding random noise. When this noise typically has a zero mean and and insufficient variance, an adversary can recover the underlying model parameters using simple techniques such as sliding-window averaging. A recent method using masked diffusion attempts to address this issue, but it also employs a zero-mean noise Han et al. (2025). When more zero-mean noise is injected, a small forgetting factor becomes necessary to mitigate its adverse effects, which inevitably weakens the collaborative performance among nodes over network. Our approach takes a different direction. Instead of relying on zero-mean noise, we introduce nonzero perturbation vectors into transmission values and, more generally, employ random matrix-step-sizes for local gradients. This approach enhances privacy protection while preserving learning performance. In addition, our EDSG-RMS algorithm reduces communication overhead—each iteration requires only half as many communication rounds as the masked diffusion primal-dual stochastic gradient algorithm.

In Li et al. (2019b), the NIDS algorithm employs heterogeneous step-sizes that vary only across agents; however, each agent uses a fixed step-size over time. In contrast, our proposed algorithms introduce random matrix-valued step-sizes that vary both across agents (in space) and across iterations (in time). Consequently, every agent utilizes a distinct step-size at each iteration, ensuring that even if the average step-size used by an agent is disclosed, the actual gradient information remains protected. While the work in Wan et al. (2023) also leverages random step-sizes for gradient protection, it operates within a federated learning framework—a centralized setting—and does not provide convergence analysis. Our work focuses on a fully decentralized setting (in both homogeneous and heterogeneous networks) and includes rigorous convergence guarantees for both convex and strongly convex objectives.

108 3 BACKGROUND AND MOTIVATION
109110 Consider the following distributed optimization problem over an undirected network:
111

112
$$\min_{w \in \mathbb{R}^L} J(w) = \frac{1}{K} \sum_{k=1}^K J_k(w), \quad (1)$$

113
114

115 where K is the number of networked agents, $J_k(w)$ is the convex local risk function at agent k .
116117 3.1 DSG AND EDSG ALGORITHMS
118119 To solve the problem in a distributed manner, we consider the following two algorithms.
120121 3.1.1 DSG ALGORITHM
122123 At agent k , the DSG is executed as
124

125
$$\begin{cases} \psi_k(n) = \mathbf{w}_k(n-1) - \gamma \widehat{\nabla J}_k(\mathbf{w}_k(n-1); \mathbf{x}_k(n)), & \text{(local update)} \\ \mathbf{w}_k(n) = \sum_{\ell \in \mathcal{N}_k} a_{\ell k} \psi_{\ell}(n), & \text{(combination)} \end{cases} \quad (2a)$$

126
127

128
$$\begin{cases} \psi_k(n) = \mathbf{w}_k(n-1) - \gamma \widehat{\nabla J}_k(\mathbf{w}_k(n-1); \mathbf{x}_k(n)), & \text{(local update)} \\ \mathbf{w}_k(n) = \sum_{\ell \in \mathcal{N}_k} a_{\ell k} \psi_{\ell}(n), & \text{(combination)} \end{cases} \quad (2b)$$

129 for $n \geq 1$, where the initial weight $\mathbf{w}_k(0)$ can be any finite value, $\gamma > 0$ is a deterministic step-
130 size, $A = [a_{\ell k}]$ is a symmetric and doubly stochastic combination matrix, $\widehat{\nabla J}_k(\mathbf{w}_k(n-1); \mathbf{x}_k(n))$
131 represents the stochastic gradient using sample $\mathbf{x}_k(n)$, and \mathcal{N}_k denotes the set of neighboring agents
132 for agent k , including itself.133 3.1.2 EDSG ALGORITHM
134135 At agent k , the update of EDSG is
136

137
$$\begin{cases} \psi'_k(n) = \mathbf{w}'_k(n-1) - \gamma \widehat{\nabla J}_k(\mathbf{w}'_k(n-1); \mathbf{x}_k(n)), & \text{(local update)} \\ \phi'_k(n) = \psi'_k(n) + \mathbf{w}'_k(n-1) - \psi'_k(n-1), & \text{(correction)} \end{cases} \quad (3a)$$

138
139

140
$$\begin{cases} \mathbf{w}'_k(n) = \sum_{\ell \in \mathcal{N}_k} a_{\ell k} \phi'_{\ell}(n), & \text{(combination)} \end{cases} \quad (3c)$$

141

142 for $n \geq 1$, where $A = [a_{\ell k}]$ is another symmetric and doubly stochastic combination matrix¹. The
143 initial values are set as $\psi'_k(0) = \mathbf{w}'_k(0)$, where $\mathbf{w}'_k(0)$ can take any finite value.
144145 The DSG and EDSG algorithms belong to the well-established classes of primal and primal-dual
146 methods, respectively. Compared to gradient tracking algorithms, both exhibit lower communication
147 overhead, as each iteration entails only a single round of variable exchange among agents. This
148 communication efficiency motivates our focus on these two algorithms. Moreover, as demonstrated
149 in Sayed (2022), EDSG generally outperforms DSG in heterogeneous data settings, whereas DSG
150 tends to be more effective when the data across agents is homogeneous.151 3.2 PRIVACY ISSUES DISCUSSION
152153 We now examine the privacy issues of these two algorithms under two types of adversaries: external
154 eavesdroppers and honest-but-curious internal agents. External eavesdroppers are passive adver-
155 saries located outside the network who intercept communication links to infer agents' estimated
156 parameters, local gradients, and potentially their private training data. Honest-but-curious agents
157 faithfully execute the algorithm but may misuse the information received during collaboration to
158 infer sensitive data—such as gradients or training samples—belonging to their neighbors. In both
159 cases, we assume that both types of adversaries have full knowledge of the combination matrix used
160 in the consensus step.161 ¹The matrix A in (3) is positive-definite, as detailed in Sayed (2022).

162 3.2.1 PRIVACY RISKS ASSOCIATED WITH $w_k(n)$ AND $w'_k(n)$
163164 If the sequences $\{\psi_\ell(n)\}$ or $\{\phi'_\ell(n)\}$ is accessible to external eavesdroppers for $n = 1, 2, \dots, N$
165 and $\ell = 1, 2, \dots, K$, then the values $\{\mathbf{w}_k(n), n = 1, 2, \dots, N\}$ and $\{\mathbf{w}'_k(n), n = 1, 2, \dots, N\}$
166 can be derived using (2b) and (3c). This exposure could lead to the unintended disclosure of sensi-
167 tive network estimation, for instance, the leakage of location information in distributed localization
168 systems.169 3.2.2 PRIVACY RISKS IN LOCAL GRADIENT INFORMATION
170171 If honest-but-curious agents have access to $\{\psi_\ell(n)\}$ or $\{\phi'_\ell(n)\}$ for $n = 1, 2, \dots, N$ and $\ell =$
172 $1, 2, \dots, K$, they can infer local gradient information using the relationships $\gamma \widehat{\nabla J}_\ell(\mathbf{w}_\ell(n); \mathbf{x}_\ell(n +$
173 $1)) = \mathbf{w}_\ell(n) - \psi_\ell(n+1)$ and $\gamma \widehat{\nabla J}_\ell(\mathbf{w}'_\ell(n); \mathbf{x}_\ell(n+1)) = \mathbf{w}'_\ell(n) - \phi'_\ell(n+1)$ for $n = 2, 3, \dots, N-1$.
174 Then, honest-but-curious agents, knowing the step-size parameter γ , can accurately reconstruct gra-
175 dient information from neighboring agents. External eavesdroppers, however, would obtain gradi-
176 ents with an unknown amplitude scaling.177 In distributed least-mean-square (LMS) filtering Sayed (2014), the local gradient at time n is ex-
178 pressed as $\gamma(\mathbf{d}_k(n) - \mathbf{x}_k^\top(n) \mathbf{w}) \mathbf{x}_k(n)$, where $\mathbf{x}_k(n)$ represents the local data. This gradient is
179 a scaled version of the local data, which means that external eavesdroppers may extract sensitive
180 information about the underlying data.182 3.2.3 PRIVACY RISKS IN LOCAL DATA EXPOSURE
183184 In deep learning, a honest-but-curious agent who has access to both the gradient
185 $\widehat{\nabla J}_k(\mathbf{w}_k(n); \mathbf{x}_k(n+1))$ and model parameter $\mathbf{w}_k(n)$ can leverage model inversion inference tech-
186 niques, such as those proposed in Zhu et al. (2019), to reconstruct the local training data. Conse-
187 quently, in the standard DSG and EDSG algorithms, local training data may be inadvertently leaked.189 4 PROPOSED METHODS
190191 To address the privacy concerns discussed, this section introduces the DSG-RMS and EDSG-RMS
192 algorithms. We then present their mean-square stability and privacy analysis, followed by a discus-
193 sion of an efficient approach for selecting matrix step-sizes with reduced computational complexity.195 4.1 PROPOSED ALGORITHMS
196197 We begin by defining a random matrix $\mathbf{M}_k(n)$, constructed as follows:

198
$$\mathbf{M}_k(n) = \begin{bmatrix} \boldsymbol{\mu}_{k1}(n) & & \mathbf{Z}_k(n) \\ & \boldsymbol{\mu}_{k2}(n) & \\ \mathbf{Z}'_k(n) & \ddots & \boldsymbol{\mu}_{kL}(n) \end{bmatrix}, \quad L \times L \quad (4)$$

200
201
202

203 where the blocks $\mathbf{Z}_k(n)$ and $\mathbf{Z}'_k(n)$ consist of elements with zero mean, while the main diagonal
204 elements $\{\boldsymbol{\mu}_{k\ell}(n), \ell = 1, 2, \dots, L\}$ share a common mean value $\mu > 0$. Each element in the random
205 matrix may have a different variance.206 Using this random matrix, we develop the following algorithms.
207

208 • (DSG-RMS)

209
$$\begin{cases} \psi_k(n) = \mathbf{w}_k(n-1) - \gamma \mathbf{M}_k(n) \widehat{\nabla J}_k(\mathbf{w}_k(n-1); \mathbf{x}_k(n)), & \text{(local update)} \end{cases} \quad (5a)$$

210
211

$$\begin{cases} \psi_k^c(n) = \psi_k(n) + \frac{\tau}{\sqrt{L}} \mathbf{c}_k(n-1), & \text{(protection)} \end{cases} \quad (5b)$$

212
213

$$\begin{cases} \mathbf{w}_k(n) = \sum_{\ell \in \mathcal{N}_k} a_{\ell k} \psi_\ell^c(n) - \psi_k^c(n) + \psi_k(n), & \text{(combination)} \end{cases} \quad (5c)$$

214
215

where $\mathbf{c}_k(n-1) = \|\mathbf{w}_k(n-1)\| \cdot \mathbb{1}_L$ and $\tau \neq 0$ is a free parameter.

216 • (EDSG-RMS)

218
$$\begin{cases} \psi'_k(n) = \mathbf{w}'_k(n-1) - \gamma \mathbf{M}_k(n) \widehat{\nabla J}_k(\mathbf{w}'_k(n-1); \mathbf{x}_k(n)), & \text{(local update)} \\ \phi'_k(n) = \psi'_k(n) + \mathbf{w}'_k(n-1) - \psi'_k(n-1), & \text{(correction)} \\ \phi'^c_k(n) = \phi'_k(n) + \frac{\tau}{\sqrt{L}} \mathbf{c}'_k(n-2), & \text{(protection)} \\ \mathbf{w}'_k(n) = \sum_{\ell \in \mathcal{N}_k} a_{\ell k} \phi'^c_{\ell}(n) - \phi'^c_k(n) + \phi'_k(n), & \text{(combination)} \end{cases} \quad (6a)$$

219
$$(6b)$$

220
$$(6c)$$

221
$$(6d)$$

222 where $\mathbf{c}'_k(n) = \|\mathbf{w}'_k(n)\| \cdot \mathbb{1}_L$ and the initial value $\mathbf{c}'_k(-1)$ is set to a random vector.

223 In (5b) and (6c), $\mathbf{c}_k(n-1)$ and $\mathbf{c}'_k(n-2)$ serve as data protection vectors, which protect transmission
224 values $\psi_k(n)$ and $\phi'_k(n)$, respectively. Increasing the parameter τ strengthens this protection but
225 may affect the stability of the algorithm. Theorems 1 and 2 specify the effective range of τ . At each
226 time step n , $\gamma \mathbf{M}_k(n)$ works as random matrix-step-sizes, with its expected value given by $\gamma \mu \mathbf{I}_L$.
227 In the EDSG-RMS algorithm, we use $\mathbf{c}'_k(n-2)$ instead of $\mathbf{c}'_k(n-1)$, primarily to facilitate the
228 theoretical analysis of the algorithm.

229 **Remark 1 (Protection mechanisms)** During the local update phase, the random matrix $\mathbf{M}_k(n)$
230 serves as a form of multiplicative noise that modifies the gradient information. This matrix is locally
231 generated and remains private to each agent, thereby helping to obscure the true stochastic gradient
232 and reduce the risk of model inversion attacks. In the protection step, a dynamic non-zero vector
233 is added to the transmission vector to prevent inference attacks based on statistical analysis, such
234 as estimating the mean of network updates. Beyond the protection vector form in (5b), alternative
235 formulations can be employed, such as $\tau \operatorname{erf}(0.1 \mathbf{w}_k(n-1))$ and $\tau \tanh(\mathbf{w}_k(n-1))$, where $\operatorname{erf}(\cdot)$
236 and $\tanh(\cdot)$ denote the error and hyperbolic tangent functions, respectively.²

237 **Remark 2 (Method extension)** The multiplicative noise $\mathbf{M}_k(n)$ in (5a), protection mechanism (5b),
238 and combination step (5c) can be integrated into gradient tracking type algorithms to ensure privacy
239 protection. However, unlike the algorithms (5) and (6), which require only one communication round
240 per iteration, the gradient tracking algorithm necessitates two rounds per iteration.

241 4.2 CONVERGENCE AND PRIVACY ANALYSIS

242 **Assumption 1 (Network topology)** The undirected network is strongly-connected. If agents ℓ and k
243 are linked, then $a_{\ell k} > 0$; otherwise $a_{\ell k} = 0$, where A is a symmetric and doubly stochastic matrix.

244 **Strong connectedness means that, for any pair of agents, there exists an undirected path with positive
245 edge weights connecting them, and moreover, at least one agent has a positive self-loop (i.e., $a_{kk} > 0$, for some k).** The combination matrix $\mathcal{A} = A \otimes \mathbf{I}_L$ can be decomposed as follows: Sayed (2022)

246
$$\mathcal{A} = \underbrace{[K\Gamma, c\mathcal{X}_R]}_{\mathcal{X}} \underbrace{\begin{bmatrix} \mathbf{I}_L & \mathbf{0} \\ \mathbf{0} & \mathcal{D} \end{bmatrix}}_{\Sigma} \underbrace{\begin{bmatrix} \Gamma^T \\ \frac{1}{c}\mathcal{X}_L \end{bmatrix}}_{\mathcal{X}^{-1}}, \quad (7)$$

247 where $\Gamma = \frac{1}{K} \mathbb{1}_K \otimes \mathbf{I}_L$, $\mathcal{D} = \operatorname{diag}\{\lambda_2, \dots, \lambda_K\} \otimes \mathbf{I}_L$, and $c > 0$. The eigenvalues $\{\lambda_2, \dots, \lambda_K\}$
248 exclude 1. For DSG-RMS, $-1 < \lambda_\ell < 1$; for EDSG-RMS, $0 < \lambda_\ell < 1$ ($\ell = 2, \dots, K$). Here, \mathbf{I}_L
249 and $\mathbb{1}_K$ denotes $L \times L$ identity matrix and $K \times 1$ all one vector, respectively.

250 **Assumption 2 (Gradient noise)** For any agent k and time n , the gradient noise $\mathbf{s}_{k,n}(\mathbf{w}) =$
251 $\widehat{\nabla J}_k(\mathbf{w}; \mathbf{x}_k(n)) - \nabla J_k(\mathbf{w})$ is temporally and spatially independent, and satisfies

252
$$\mathbb{E}\{\mathbf{s}_{k,n}(\mathbf{w}) | \mathcal{F}_{n-1}\} = \mathbf{0}, \quad \mathbb{E}\{\|\mathbf{s}_{k,n}(\mathbf{w})\|^2 | \mathcal{F}_{n-1}\} \leq \sigma_{s,k}^2, \quad (8)$$

253 where $\mathbf{w} \in \mathcal{F}_{n-1}$, $\sigma_{s,k}^2 \geq 0$, and $\mathcal{F}_{n-1} = \text{filtration}\{\mathbf{w}_k(0), \dots, \mathbf{w}_k(n-1), \text{all } k\}$.

254 ²The mean-square error analysis for these alternatives can be conducted using inequalities $|\operatorname{erf}(0.1x) - \operatorname{erf}(0.1y)|^2 \leq 0.1|x - y|^2$ and $|\tanh(x) - \tanh(y)|^2 \leq |x - y|^2$.

270 **Assumption 3 (Random matrix-step-sizes)** For each agent k and time n , $\mathbf{M}_k(n)$ has mutually
 271 independent entries, which are also independent across both time and agents. Its ℓ -th diagonal
 272 element $\mu_{k,\ell}(n)$ satisfies

$$274 \quad \mathbb{E}\{\mu_{k,\ell}(n)\} \triangleq \mu, \quad \mathbb{E}\{(\mu_{k,\ell}(n) - \mu)^2\} \triangleq \sigma_{\mu,k}^2, \quad (9)$$

275 with constants $\mu > 0$, $\sigma_{\mu,k} > 0$. Off-diagonal entries are zero-mean with variances bounded by σ_z^2 .

277 It follows that $\mathbb{E}\{\mathbf{M}_k(n)\} = \mu\mathbf{I}_L$, $\mathbb{E}\{\|\mathbf{M}_k(n) - \mu\mathbf{I}_L\|^2\} \leq \sigma_\mu^2$, and $\mathbb{E}\{\|\mathbf{M}_k(n)\|^2\} \leq \theta_\mu^2$, where
 278 $\sigma_\mu^2 = \max\{\sigma_{\mu,k}^2 + (L-1)\sigma_z^2, k = 1, 2, \dots, K\}$ and $\theta_\mu^2 = \max\{\mu^2 + \sigma_{\mu,k}^2 + (L-1)\sigma_z^2, k = 1, 2, \dots, K\}$. Unlike Zhao & Sayed (2014); Han et al. (2025), the variables $\{\mu_{k,\ell}(n)\}$ may take
 279 negative values.

280 **Assumption 4 (Lipschitz continuous gradient)** Each risk function $J_k(w)$ is δ -smooth:

$$282 \quad \|\nabla J_k(x) - \nabla J_k(y)\| \leq \delta\|x - y\|, \quad \forall x, y \in \mathbb{R}^L \quad (10)$$

285 for some positive constant δ . Additionally, the network cost function $J(w) = \frac{1}{K} \sum_{k=1}^K J_k(w)$ is
 286 lower bounded, i.e., $J(w) \geq J^*$, where J^* denotes the optimal value of $J(w)$.

288 **Assumption 5 (Convex function)** Each risk function $J_k(w)$ is convex, meaning that for any $x, y \in$
 289 \mathbb{R}^L , the following inequality holds:

$$290 \quad J_k(x) - J_k(y) + \frac{\nu}{2}\|x - y\|^2 \leq \langle \nabla J_k(x), x - y \rangle, \quad (11)$$

292 where $\nu \geq 0$ is a constant. Let w^* denote an optimal solution. If $\nu > 0$ (i.e., the function is
 293 strongly-convex), the optimal solution w^* will be unique.

295 **Theorem 1 (Convergence of DSG-RMS)** Under Assumptions 1–5, the following convergence
 296 guarantees hold.

- 298 • For the convex case ($\nu = 0$), if γ and τ satisfy

$$300 \quad \gamma \leq \frac{\mu(1 - \|\mathcal{D}\|)}{14\delta\theta_\mu^2}, \quad (12)$$

$$302 \quad |\tau| < \frac{1 - \|\mathcal{D}\|}{\sqrt{8}\|\mathcal{D} - \mathbf{I}_{(K-1)L}\|}, \quad (13)$$

304 then the time-averaged expected cost function satisfies

$$306 \quad \frac{1}{N} \sum_{n=1}^N (\mathbb{E}\{J(\bar{\mathbf{w}}_{n-1})\} - J(w^*)) \leq \frac{2\mathbb{E}\{\|\bar{\mathbf{w}}_0 - w^*\|^2\}}{\gamma\mu N} + \frac{12\delta\mathbb{E}\{\|\mathcal{W}_0\|^2\}}{N(1 - \|\mathcal{D}\|)K} \\ 307 \quad + \frac{12\gamma^2\theta_\mu^2\delta\|\mathcal{D}\|^2}{1 - \|\mathcal{D}\|} \left(\frac{8\|\nabla\mathcal{J}(\mathcal{W}^*)\|^2}{(1 - \|\mathcal{D}\|)K} + \sigma_s^2 \right) + \frac{\gamma}{\mu K} \left(\frac{8\sigma_\mu^2\|\nabla\mathcal{J}(\mathcal{W}^*)\|^2}{K} + \frac{\theta_\mu^2\sigma_s^2}{2} \right), \quad (14)$$

312 where $\bar{\mathbf{w}}_n = \Gamma^\top \mathcal{W}_n$, $\mathcal{W}_n = \text{col}\{\mathbf{w}_1(n), \mathbf{w}_2(n), \dots, \mathbf{w}_K(n)\}$, $\mathcal{W}^* = \mathbb{1}_K \otimes w^*$, and
 313 $\sigma_s^2 = \max\{\sigma_{s,k}^2, k = 1, 2, \dots, K\}$.

- 315 • For the strongly-convex case ($\nu > 0$), if τ satisfies the condition (13) and γ satisfies

$$316 \quad \gamma \leq \frac{\mu\nu(1 - \|\mathcal{D}\|)}{64\theta_\mu^2\delta^2} \sqrt{\frac{\nu}{\delta}}, \quad (15)$$

319 then the expected squared error is bounded as follows:

$$320 \quad \mathbb{E}\{\|\bar{\mathbf{w}}_n - w^*\|^2\} \leq \left(1 - \frac{\gamma\mu\nu}{8}\right)^n \left(\mathbb{E}\{\|\bar{\mathbf{w}}_0 - w^*\|^2\} + \frac{\mathbb{E}\{\|\mathcal{W}_0\|^2\}}{K} \right) \\ 321 \quad + \frac{8\gamma}{\mu\nu K} \left(\frac{4\sigma_\mu^2\|\nabla\mathcal{J}(\mathcal{W}^*)\|^2}{K} + \theta_\mu^2\sigma_s^2 \right) + \gamma^2 \frac{48\theta_\mu^2\delta\|\mathcal{D}\|^2}{\nu(1 - \|\mathcal{D}\|)} \left(\frac{8\|\nabla\mathcal{J}(\mathcal{W}^*)\|^2}{(1 - \|\mathcal{D}\|)K} + \sigma_s^2 \right). \quad (16)$$

324 *Proof:* The proof is provided in the Appendix.
 325

326 **Theorem 2 (Convergence of EDSG-RMS)** Under Assumptions 1–5, the following results hold.
 327

- 328 • For the convex case ($\nu = 0$), if γ and τ satisfy

$$329 \quad \gamma \leq \min \left\{ \frac{(1 - \|\mathcal{D}\|)\sigma_b^{0.5}}{28\delta(\sigma_\mu + \mu)}, \frac{\mu}{2\delta(2\mu^2 + \sigma_\mu^2)} \right\}, \quad (17)$$

$$330 \quad |\tau| \leq \frac{(1 - \|\mathcal{D}\|)\sigma_b^{0.5}}{\sqrt{32(1 - \sigma_b)}}, \quad (18)$$

331 where $\sigma_b = \min\{\lambda_i, i = 2, 3, \dots, K\}$, then the following convergence bound holds
 332

$$333 \quad \frac{1}{N} \sum_{n=1}^N (\mathbb{E}\{J(\bar{\mathbf{w}}'_{n-1})\} - J(w^*)) \leq \frac{2\mathbb{E}\{\|\bar{\mathbf{w}}'_0 - w^*\|^2\}}{\gamma\mu N} + \frac{48\delta(3 - \|\mathcal{D}\|)\mathbb{E}\{\|\mathcal{W}'_0\|^2\}}{NK(1 - \|\mathcal{D}\|)^2} \\ 334 \quad + \frac{96\gamma^2\mu^2\delta}{NK} \frac{\mathbb{E}\{\|\nabla\mathcal{J}(\bar{\mathcal{W}}'_0)\|^2\}}{(1 - \|\mathcal{D}\|)^2} + \frac{144\gamma^2\delta\|\mathcal{D}\|^2}{(1 - \|\mathcal{D}\|)} \left(\frac{3\sigma_\mu^2\|\nabla\mathcal{J}(\mathcal{W}^*)\|^2}{(1 - \|\mathcal{D}\|)K} + \theta_\mu^2\sigma_s^2 \right) \\ 335 \quad + \frac{2\gamma}{\mu K} \left(\frac{4\sigma_\mu^2}{K} \|\nabla\mathcal{J}(\mathcal{W}^*)\|^2 + \theta_\mu^2\sigma_s^2 \right), \quad (19)$$

336 where $\bar{\mathbf{w}}'_n = \Gamma^\top \mathcal{W}'_n$, $\mathcal{W}'_n = \text{col}\{\mathbf{w}'_1(n), \mathbf{w}'_2(n), \dots, \mathbf{w}'_K(n)\}$, and $\bar{\mathcal{W}}'_n = (\frac{1}{K}\mathbb{1}_K\mathbb{1}_K^\top \otimes$
 337 $\mathbf{I}_L)\mathcal{W}'_n$.

- 338 • For the strongly-convex case ($\nu > 0$), if τ satisfies the condition (18) and γ satisfies

$$339 \quad \gamma \leq \min \left\{ \frac{(1 - \|\mathcal{D}\|)\sigma_b^{0.5}}{40(\sigma_\mu + \mu)\delta} \sqrt{\frac{\nu}{\delta}}, \frac{\mu\nu(1 - \|\mathcal{D}\|)}{64(\sigma_\mu^2 + \mu^2)\delta^2} \right\}, \quad (20)$$

340 then the expected squared error is bounded as follows:
 341

$$342 \quad \mathbb{E}\{\|\bar{\mathbf{w}}'_n - w^*\|^2\} \leq \left(1 - \frac{\gamma\mu\nu}{8}\right)^n \left(\mathbb{E}\{\|\bar{\mathbf{w}}_0 - w^*\|^2\} + \frac{(3 - \|\mathcal{D}\|)\mathbb{E}\{\|\mathcal{W}'_0\|^2\}}{K(1 - \|\mathcal{D}\|)} \right. \\ 343 \quad \left. + \frac{2\gamma^2\mu^2\|\nabla\mathcal{J}(\bar{\mathcal{W}}'_0)\|^2}{K(1 - \|\mathcal{D}\|)} \right) + \frac{8\gamma}{\mu\nu K} \left(\frac{4\sigma_\mu^2\|\nabla\mathcal{J}(\mathcal{W}^*)\|^2}{K} + \theta_\mu^2\sigma_s^2 \right) \\ 344 \quad + \frac{576\gamma^2\delta\|\mathcal{D}\|^2}{\nu(1 - \|\mathcal{D}\|)} \left(\frac{3\sigma_\mu^2\|\nabla\mathcal{J}(\mathcal{W}^*)\|^2}{(1 - \|\mathcal{D}\|)K} + \theta_\mu^2\sigma_s^2 \right). \quad (21)$$

345 *Proof:* The detailed proof can be found in the Appendix.
 346

347 **Remark 3 (Impact of protection vector and random matrix-step-sizes)** The parameter τ does not
 348 affect steady-state performance, while σ_μ^2 does. The impact grows with data heterogeneity (caused
 349 by $\|\nabla\mathcal{J}(\mathcal{W}^*)\|^2$ in the bounds). Choosing a smaller γ can improve network estimation accuracy.
 350

351 **Remark 4 (Sparsely connected network)** In sparsely connected networks ($\|\mathcal{D}\|^2 \rightarrow 1$), the terms
 352 $O(\gamma^2\theta_\mu^2\|\mathcal{D}\|^2/(1 - \|\mathcal{D}\|)^2)$ in DSG-RMS and $O(\gamma^2\sigma_\mu^2\|\mathcal{D}\|^2/(1 - \|\mathcal{D}\|)^2)$ in EDSG-RMS strongly
 353 affect steady-state performance. Since $\theta_\mu^2 > \sigma_\mu^2$, EDSG-RMS can achieve better steady-state per-
 354 formance than DSG-RMS.
 355

356 Define the mutual information $I(X; Y)$, which measures the amount of information learned about X
 357 by observing Y (Cover (1999); Li et al. (2020)). Then, we have privacy-preserving results for network
 358 estimation and gradients.

359 **Theorem 3 (Privacy of Network Estimates and Gradients)** Consider the setting where all ran-
 360 dom step-sizes share the same variance σ_μ^2 . Then, $\lim_{\sigma_\mu^2 \rightarrow \infty} I(S_k(n); Z_k(n)) = 0$, where
 361

378 $S_k(n) = \widehat{\nabla J}_k(\mathbf{w}_k(n-1); \mathbf{x}_k(n))$, $Z_k(n) = \mathbf{M}_k(n) \widehat{\nabla J}_k(\mathbf{w}_k(n-1); \mathbf{x}_k(n))$, and $\mathbf{M}_k(n)$ denotes the random step-size applied by agent k at time n . In addition, for an external eavesdropper, even upon observing a large number of intermediate variables $\psi_k^c(n)$, the eavesdropper remains unable to reconstruct the network's estimate without knowledge of τ .

382 *Proof:* By computing the mutual information between the private gradient and the observed signal
 383 under multiplicative noise, the desired result follows directly. The proof proceeds analogously to the
 384 analysis of additive noise perturbation in Li et al. (2020).

386 **Remark 5 (Trade-off between privacy and algorithm convergence speed)** According to Theorem 3,
 387 gradient information leakage can be effectively suppressed by choosing a sufficiently large variance
 388 for the random step-sizes. However, Theorems 1 and 2 indicate that increasing the variance de-
 389 grades the network's estimation accuracy. Fortunately, this degradation can be alleviated by re-
 390 ducing the parameter γ . Nevertheless, a smaller γ leads to slower convergence of the algorithm,
 391 revealing an inherent trade-off between privacy preservation and algorithm convergence speed. The
 392 trade-off can be alleviated, by adopting a time-varying strategy $\gamma(k)$ that gradually decreases over
 393 iterations.

394 4.3 LOW-COMPLEXITY CHOICE OF MATRIX-STEP-SIZE

396 When all elements of $\mathbf{M}_k(n)$ are non-zero, computing $\mathbf{M}_k(n) \widehat{\nabla J}_k(\mathbf{w}_k(n-1); \mathbf{x}_k(n))$ requires
 397 $O(L^2)$ operations. To reduce this cost, we propose two sparse alternatives for $\mathbf{M}_k(n)$:

- 399 • Upper Triangular Structure: $\mathbf{M}_k(n)$ is constrained to the following upper triangular form:

$$400 \quad \mathbf{M}_k(n) = \begin{bmatrix} \mu_{k1}(n) & \star_1 & 0 & 0 \\ 401 & 0 & \mu_{k2}(n) & \star_2 \\ 402 & \vdots & \vdots & \ddots & \star_{L-1} \\ 403 & 0 & 0 & 0 & \mu_{kL}(n) \end{bmatrix}, \quad (22)$$

406 where \star_ℓ represents non-zero elements;

- 407 • Sparse Randomized Structure: In addition to the diagonal elements, L off-diagonal entries
 408 are randomly selected and assigned values drawn from zero-mean random variables.

410 In both cases, the complexity of computing $\mathbf{M}_k(n) \widehat{\nabla J}_k(\mathbf{w}_k(n-1); \mathbf{x}_k(n))$ is reduced to $O(L)$.

412 5 EXPERIMENTAL VERIFICATION

414 In all algorithms, the initial estimates are drawn uniformly from $[-1, 1]$. The network in-
 415 cludes five agents with randomly generated links satisfying Assumption 1, and combination ma-
 416 trices are built using the Laplacian rule. Performance is measured by the mean-square devia-
 417 tion (MSD) and the squared gradient norm: $MSD(n) = \frac{1}{K} \sum_{k=1}^K \|\mathbf{w}_k(n) - \mathbf{w}^*\|^2$, $\|\nabla J\|^2(n) =$
 418 $\frac{1}{n} \sum_{\ell=1}^n \|\nabla J(\mathbf{w}_{\ell-1})\|^2$.

420 5.1 APPLICATION: ADAPTIVE FILTERING

422 We consider a linear adaptive filtering task where each agent observes streaming data $\mathbf{d}_k(n) =$
 423 $\mathbf{x}_k^\top(n) \mathbf{w}_k^o + \mathbf{v}_k(n)$, $k = 1, 2, \dots, K$, with local optimum \mathbf{w}_k^o and zero-mean noise $\mathbf{v}_k(n)$. For
 424 Gaussian noise $\mathbf{v}_k(n)$, the global optimum of the network MSE cost, $\min \frac{1}{2K} \sum_{k=1}^K \mathbb{E} \{(\mathbf{d}_k(n) -$
 425 $\mathbf{x}_k^\top(n) \mathbf{w})^2\}$, is $\mathbf{w}^* = (\sum_{k=1}^K R_{x,k})^{-1} (\sum_{k=1}^K R_{x,k} \mathbf{w}_k^o)$, where $R_{x,k} = \mathbb{E} \{\mathbf{x}_k(n) \mathbf{x}_k^\top(n)\}$. In the
 426 simulation, $\mathbf{x}_k(n) \sim \mathcal{N}(0, \sigma_{x,k}^2 \mathbf{I}_5)$, $\mathbf{v}_k(n) \sim \mathcal{N}(0, \sigma_{v,k}^2)$, and $\mathbf{w}_k^o \sim \mathcal{N}(0, \mathbf{I}_5)$, with $\sigma_{x,k}^2, \sigma_{v,k}^2 \sim$
 427 $\mathcal{U}(0, 1)$. To test the tracking, \mathbf{w}_k^o changes sign during intermediate iterations. Fig. 1 shows con-
 428 vergence curves of DSG-RMS and EDSG-RMS under homogeneous and heterogeneous networks,
 429 using both stochastic and exact gradients. In Fig. 1(c), the notations $\psi_{k,1}(n)$, $\mathbf{w}_{k,1}(n-1)$, $\psi_{k,1}^c(n)$,
 430 and w_1^* refer to the first elements of $\psi_k(n)$, $\mathbf{w}_k(n-1)$, $\psi_k^c(n)$, and w^* , respectively. Parameters are
 431 set to $\gamma = 0.0001$, $\mu = 1$, $\tau = 1$, and $\sigma_z^2 = 0.0001$ for DSG-RMS/EDSG-RMS. For PD-LMSRizk

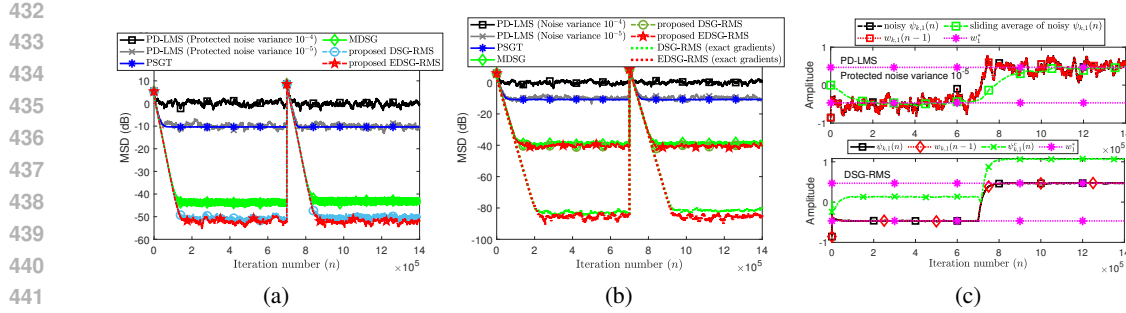


Figure 1: Convergence of DSG-RMS and EDSG-RMS compared with PD-LMS Rizk et al. (2023), PSGT Ding et al. (2021), and MDSGHan et al. (2025). (a) MSD curves (10 runs) on a homogeneous network ($w_1^o = \dots = w_K^o$); (b) MSD curves (10 runs) on a heterogeneous network ($w_1^o \neq \dots \neq w_K^o$); (c) Convergence curves (1 run) of $\psi_{k,1}(n)$, $w_{k,1}(n-1)$, and $\psi_{k,1}^c(n)$ in Fig. 1(b) at agent $k = 1$.

et al. (2023), PSGT Ding et al. (2021), and MDSGHan et al. (2025), the protection noise variances are 0.0001 , $\sqrt{0.1 \cdot 0.8^n}$, and 0.0001 , respectively.³ As a comparison, the MSD curve of PD-LMS using a protection noise variance 10^{-5} is included. As shown in Fig. 1, our algorithms outperform the comparison methods in terms of convergence performance, and effectively prevent external agents from inferring the network estimate through sliding averages. For PD-LMS with protection noise variance 10^{-5} , an eavesdropper can approximate the target parameters via averaging, as seen in Fig. 1(c). When the protection noise variance is increased to 10^{-4} , the PD-LMS fails to estimate the model parameters, under the network parameter settings. Moreover, under heterogeneous data, EDSG-RMS outperforms DSG-RMS when both use exact gradients, as illustrated in Fig. 1(b).

5.2 APPLICATION: DISTRIBUTED LEARNING

In the second experiment, we evaluate the proposed strategies by collaboratively training a convolutional neural network (CNN) over a random network of five agents. The MNIST dataset is evenly divided among the agents, with each missing two digit classes: agent 1 (0, 1), agent 2 (2, 3), agent 3 (4, 5), agent 4 (6, 7), and agent 5 (8, 9). The CNN consists of three convolutional layers (each with 5×5 kernels, 12 filters, and Sigmoid activations), followed by a fully connected layer that outputs 10 classes. Training uses cross-entropy loss Zhang & Sabuncu (2018), $\min -\frac{1}{K} \sum_{k=1}^K \frac{1}{N_k} \sum_{n=1}^{N_k} \sum_{\ell=1}^{10} y_{k\ell,n} \log(\hat{y}_{k\ell,n})$, where N_k is the number of samples, and $y_{k\ell,n}$, $\hat{y}_{k\ell,n}$ denote the true label and predicted probability for class ℓ of the n -th sample at agent k . Each agent randomly selects a sample at each iteration to compute a stochastic gradient for parameter updates. Other settings include protection noise variance $\sigma_{z,k}^2 = 10^{-2}$ for DSG-RMS and EDSG-RMS, $\gamma = 0.02$, $\mu = 1$, and $\tau = 0.1$. We assume agent 1 is honest-but-curious: it follows the protocol but attempts to infer agent 2's local data using the DLG attack Zhu et al. (2019), leveraging available weight and gradient estimates. For the DSG and DSG-RMS, the estimated weights and gradient informations are $\{w_2(n-1), (-\psi_2(n) + w_2(n-1))/\gamma\}$ and $\{\hat{w}_2(n-1), (-\psi_2^c(n-1) + \frac{\tau}{\sqrt{L}}\|w_1(n-1)\| \cdot \mathbb{1}_L + \hat{w}_2(n-1))/\gamma\}$, respectively, where $\hat{w}_2(n) \approx \sum_{\ell \in \mathcal{N}_2} a_{\ell 2} \psi_{\ell}^c(n) - \frac{\tau}{\sqrt{L}}\|w_1(n-1)\| \cdot \mathbb{1}_L$. Due to the interplay between the correction, protection, and combination steps in the EDSG-RMS, agent 1 is unable to estimate $\psi_2'(n)$ when the initial values $c_2'(-1)$ and $w_2'(0)$ are randomly selected. In this case, the agent lacks access to the required gradient information. To test the protective role of the random matrix, we applied $w_2'(n-1)$ and $M_2(n) \widehat{\nabla J}_2(w_2'(n-1); \mathbf{x}_2(n))$ in DLG diagnosis under the EDSG-RMS. As shown in Fig. 2(a), the squared gradient norm and prediction accuracy of the proposed methods are comparable to DSG. Fig. 2(b) demonstrates that our methods are more effective at mitigating DLG attacks.

5.3 APPLICATION: TARGET LOCALIZATION

Let the unknown target location in the Cartesian plane be $w^* = [w_1^*, w_2^*]^\top$. Four anchor agents at $p_k = [x_k, y_k]^\top$, $k = 1, 2, 3, 4$, obtain noisy measurements of the distance $r_k(n)$ and direction

³PD-LMS here is a local differential privacy version, where the noise is added to each agent.

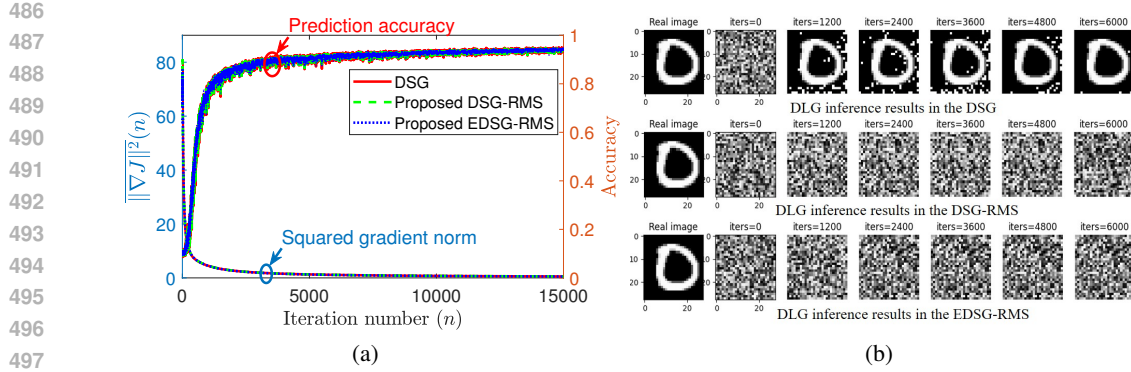


Figure 2: (a) Convergence curves (1 run) of DSG-RMS and EDSG-RMS with $\gamma = 0.02$; (b) Inference results from the DLG.

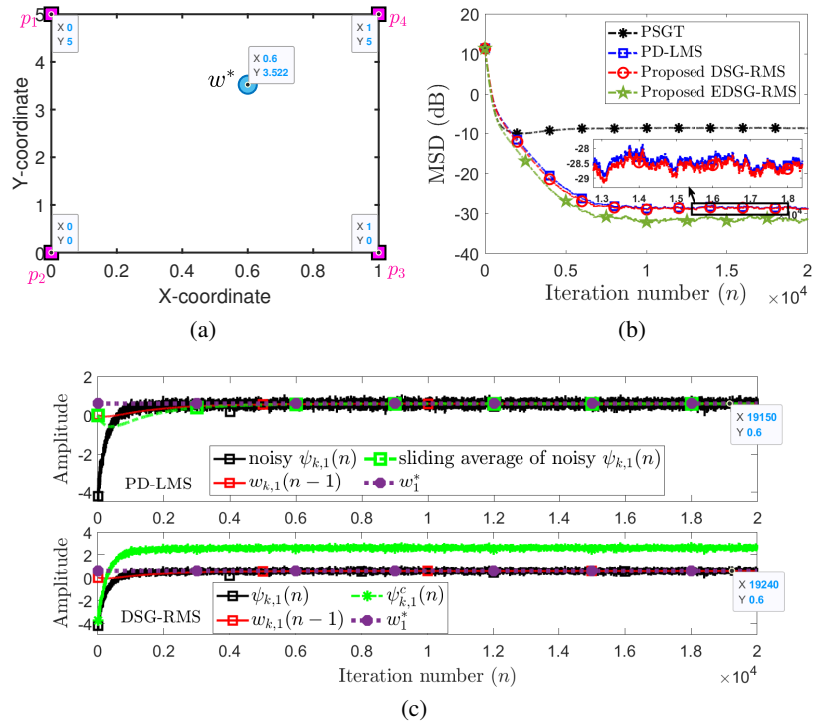


Figure 3: Convergence curves (100 runs) in target localization task. (a) localization of target and anchor agents; (b) MSD curves; (c) The changes in specific variables at agent $k = 1$.

$z_k(n)$ to the target at time n . The localization model in Sayed (2014) expresses the relationship as: $\mathbf{d}_k(n) = \mathbf{r}_k(n) + \mathbf{z}_k^\top(n)p_k = \mathbf{z}_k^\top(n)w^* + \mathbf{v}_k(n)$, $k = 1, 2, 3, 4$, where $\mathbf{v}_k(n)$ is zero-mean Gaussian noise. To estimate w^* , agents share the estimated values with neighbors. Direct sharing, however, risks exposing location information. To address this, EDSG-RMS and DSG-RMS are applied. The results, shown in Figs. 3(b) and (c), were obtained with parameters $\gamma = 4$, $\mu = 1$, $\tau = 0.8$, and $\sigma_z^2 = 0.001$. As observed, the EDSG-RMS algorithm slightly outperforms the others. The DSG-RMS and PD-LMS algorithms achieve similar performance, but the DSG-RMS and EDSG-RMS provide better privacy protection. This is because the sliding average result of the transmitted values in the PD-LMS can approximate the target location information, shown in Fig. 3(c).

6 CONCLUSION

This paper has introduced two privacy-preserving decentralized learning algorithms, DSG-RMS and EDSG-RMS, designed to mitigate information leakage in both network-estimated values and local

540 gradients/data. We have also established their convergence guarantees for convex objectives, explicit
 541 accounting for the network estimation accuracy and privacy-preserving effects of non-zero protec-
 542 tion vectors and random matrix-step-sizes. Our analysis reveals a fundamental trade-off: while in-
 543 creasing the variance of the step-size enhances gradient privacy, it inevitably degrades network esti-
 544 mation accuracy. However, this degradation can be effectively mitigated by reducing the algorithmic
 545 parameter γ . Finally, applications in distributed filtering, learning, and target localization demon-
 546 strate the effectiveness of these algorithms, highlighting their practical value in privacy-sensitive
 547 optimization.

548

549 REFERENCES

550

551 Sulaiman A Alghunaim and Kun Yuan. A unified and refined convergence analysis for non-convex
 552 decentralized learning. *IEEE Transactions on Signal Processing*, 70:3264–3279, 2022.

553 Thomas M Cover. *Elements of information theory*. John Wiley & Sons, 1999.

554 Tie Ding, Shanying Zhu, Jianping He, Cailian Chen, and Xinping Guan. Differentially private
 555 distributed optimization via state and direction perturbation in multiagent systems. *IEEE Trans-*
 556 *actions on Automatic Control*, 67(2):722–737, 2021.

557

558 Xingquan Fu, Guanghui Wen, Mengfei Niu, and Wei Xing Zheng. Distributed secure filtering
 559 against eavesdropping attacks in sinr-based sensor networks. *IEEE Transactions on Information*
 560 *Forensics and Security*, 19:3483–3494, 2024.

561

562 Hongyu Han, Sheng Zhang, Hongyang Chen, and Ali H Sayed. Masked diffusion strategy for
 563 privacy-preserving distributed learning. *IEEE Transactions on Information Forensics and Secu-*
 564 *rity*, 2025.

565 Ibrahim El Khalil Harrane, Rémi Flamary, and Cédric Richard. Toward privacy-preserving diffusion
 566 strategies for adaptation and learning over networks. In *2016 24th European Signal Processing*
 567 *Conference (EUSIPCO)*, pp. 1513–1517. IEEE, 2016.

568

569 Jianping He, Lin Cai, and Xinping Guan. Preserving data-privacy with added noises: Optimal
 570 estimation and privacy analysis. *IEEE Transactions on Information Theory*, 64(8):5677–5690,
 571 2018.

572

573 Jiahui Hu, Jiacheng Du, Zhibo Wang, Xiaoyi Pang, Yajie Zhou, Peng Sun, and Kui Ren. Does differ-
 574 ential privacy really protect federated learning from gradient leakage attacks? *IEEE Transactions*
 575 *on Mobile Computing*, 23(12):12635–12649, 2024.

576

577 Lingying Huang, Junfeng Wu, Dawei Shi, Subhrakanti Dey, and Ling Shi. Differential privacy in
 578 distributed optimization with gradient tracking. *IEEE Transactions on Automatic Control*, 69(9):
 579 5727–5742, 2024.

580

581 Qiongxiu Li, Ignacio Cascudo, and Mads Græsbøll Christensen. Privacy-preserving distributed
 582 average consensus based on additive secret sharing. In *2019 27th European Signal Processing*
 583 *Conference (EUSIPCO)*, pp. 1–5. IEEE, 2019a.

584

585 Qiongxiu Li, Richard Heusdens, and Mads Græsbøll Christensen. Privacy-preserving distributed
 586 optimization via subspace perturbation: A general framework. *IEEE Transactions on Signal*
 587 *Processing*, 68:5983–5996, 2020.

588

589 Zhi Li, Wei Shi, and Ming Yan. A decentralized proximal-gradient method with network indepen-
 590 dent step-sizes and separated convergence rates. *IEEE Transactions on Signal Processing*, 67
 591 (17):4494–4506, 2019b.

592

593 Qingguo Lü, Xiaofeng Liao, Tao Xiang, Huaqing Li, and Tingwen Huang. Privacy masking stochas-
 594 tic subgradient-push algorithm for distributed online optimization. *IEEE transactions on cyber-*
 595 *netics*, 51(6):3224–3237, 2020.

596

597 Yang Lu and Minghui Zhu. Privacy preserving distributed optimization using homomorphic encryp-
 598 tion. *Automatica*, 96:314–325, 2018.

594 Chuan Ma, Jun Li, Kang Wei, Bo Liu, Ming Ding, Long Yuan, Zhu Han, and H Vincent Poor.
 595 Trusted ai in multiagent systems: An overview of privacy and security for distributed learning.
 596 *Proceedings of the IEEE*, 111(9):1097–1132, 2023.

597

598 Payman Mohassel and Yupeng Zhang. Secureml: A system for scalable privacy-preserving machine
 599 learning. In *2017 IEEE symposium on security and privacy (SP)*, pp. 19–38. IEEE, 2017.

600 Nikos Piperigkos, Aris S Lalos, and Kostas Berberidis. Graph laplacian diffusion localization of
 601 connected and automated vehicles. *IEEE Transactions on Intelligent Transportation Systems*, 23
 602 (8):12176–12190, 2021.

603

604 Elsa Rizk, Stefan Vlaski, and Ali H Sayed. Enforcing privacy in distributed learning with perfor-
 605 mance guarantees. *IEEE Transactions on Signal Processing*, 71:3385–3398, 2023.

606 Minghao Ruan, Huan Gao, and Yongqiang Wang. Secure and privacy-preserving consensus. *IEEE*
 607 *Transactions on Automatic Control*, 64(10):4035–4049, 2019.

608

609 Ali H Sayed. Diffusion adaptation over networks. In *Academic Press Library in Signal Processing*,
 610 volume 3, pp. 323–453. Elsevier, 2014.

611

612 Ali H Sayed. *Inference and Learning from Data*, volume 1. Cambridge University Press, 2022.

613

614 Lei Shi, Wei Xing Zheng, Qingchen Liu, Yang Liu, and Jinliang Shao. Privacy-preserving dis-
 615 tributed iterative localization for wireless sensor networks. *IEEE Transactions on Industrial Elec-
 tronics*, 70(11):11628–11638, 2022.

616

617 Reza Shokri and Vitaly Shmatikov. Privacy-preserving deep learning. In *Proceedings of the 22nd*
 618 *ACM SIGSAC conference on computer and communications security*, pp. 1310–1321, 2015.

619

620 Guangnian Wan, Haitao Du, Xuejing Yuan, Jun Yang, Meiling Chen, and Jie Xu. Enhancing privacy
 621 preservation in federated learning via learning rate perturbation. In *Proceedings of the IEEE/CVF*
 622 *International Conference on Computer Vision*, pp. 4772–4781, 2023.

623

624 Kang Wei, Jun Li, Ming Ding, Chuan Ma, Howard H Yang, Farhad Farokhi, Shi Jin, Tony QS Quek,
 625 and H Vincent Poor. Federated learning with differential privacy: Algorithms and performance
 626 analysis. *IEEE transactions on information forensics and security*, 15:3454–3469, 2020.

627

628 Chunlei Zhang, Huan Gao, and Yongqiang Wang. Privacy-preserving decentralized optimization
 629 via decomposition. *arXiv preprint arXiv:1808.09566*, 2018.

630

631 Tao Zhang and Quanyan Zhu. Dynamic differential privacy for admm-based distributed classifica-
 632 tion learning. *IEEE Transactions on Information Forensics and Security*, 12(1):172–187, 2016.

633

634 Zhilu Zhang and Mert Sabuncu. Generalized cross entropy loss for training deep neural networks
 635 with noisy labels. *Advances in neural information processing systems*, 31, 2018.

636

637 Xiaochuan Zhao and Ali H Sayed. Asynchronous adaptation and learning over networks—part i:
 638 Modeling and stability analysis. *IEEE Transactions on Signal Processing*, 63(4):811–826, 2014.

639

640 Junlong Zhu, Changqiao Xu, Jianfeng Guan, and Dapeng Oliver Wu. Differentially private dis-
 641 tributed online algorithms over time-varying directed networks. *IEEE Transactions on Signal
 642 and Information Processing over Networks*, 4(1):4–17, 2018.

643

644 Ligeng Zhu, Zhijian Liu, and Song Han. Deep leakage from gradients. *Advances in neural infor-
 645 mation processing systems*, 32, 2019.

646

647